# Chapter 2

# AlterBBN

*AlterBBN* [42] was created by Alexandre Arbey in 2011, and is a public *C* program for evaluating the abundances of the elements generated during BBN. Several similar codes exists, and with the development of cosmology and nuclear physics comes the need for continuously updating the software. The first real attempt to deduct numerical experiments with the "early universe fusion reactor" came with the *Wagoner code* in 1969, based on a general numerical method published in 1968 by Robert V. Wagoner [43]. This code had a number of severe drawbacks, and was difficult to use, but it set the scene for a new era in BBN calculations. With the rapid increase in computer technology that followed, several improvements were made, and in 1988 Lawrence Kawano published the *Fortran-77* program *NUC123* [44], often referred to as the *Kawano code*. This code has later served as a reference for most of the preceding codes that have been published, and the underlying numerical methods are based on the ones laid out by Wagoner in 1968.

*AlterBBN* is structured very similar to that of *NUC123* and uses the same calculation techniques, driven by a *Runge Kutta* solver to compute the set of differential equations governing the BBN. It is also inspired by the *Fortran-77* program *PArthENoPE* [45] published in 2007, with a similar purpose as *AlterBBN*. *PArthENoPE* is a popular code for computing the BBN-created abundances, but uses a separate library (NAG) for the evaluation of some special functions and algebraic operations. This library is not included in the *PArthENoPE* package, and is quite expensive. The purpose of updating *AlterBBN* to the same standard as *PArthENoPE* is therefore to have a free, open source code that can do the same job. Moreover, some new reaction rates have been published since the release of *PArthENoPE*, which I have added to the updated *AlterBBN* code, and described later in this chapter. The source code for *PArthENoPE* can be obtained by request (but cannot be run without the NAG library), and I have used this as a reference for the implementation of the extended nuclear network.

The latest release of *AlterBBN* is *AlterBBN v1.4* of 28 June 2013 [1]. In the following I will refer to this as *the original code*. The program predicts the abundances of the light elements for various cosmological models, that can be compared to observations. It consists of five main programs which, except from the standard cosmological model program, requires that the different free parameters are given as input arguments. The five different programs are:

- **stand_cosmo.x**, which computes the abundances of the elements in the standard ΛCDM cosmological model, with a pre-defined default value of $\eta$;
- **alter_eta.x**, which computes the abundance of the elements in the standard cosmological model,

[1] May be downloaded from `http://superiso.in2p3.fr/relic/alterbbn`

with the required input argument
  - $\eta$: baryon-to-photon ratio;

- **alter_neutrinos.x**, which computes the abundance of the elements in the standard cosmological model, with the required input argument
  - $N_\nu$: the number of neutrino families,

  and the optional arguments
  - $\xi_{\nu_e}$: the electron neutrino degeneracy parameter,
  - $\xi_{\nu_\mu}$: the muon neutrino degeneracy parameter,
  - $\xi_{\nu_\tau}$: the tau neutrino degeneracy parameter;

- **alter_standmod.x**, which computes the abundance of the elements in cosmological scenarios with modified expansion rates and entropy contents, with the required arguments
  - $\kappa_\rho$: the ratio of dark energy density over radiation energy density at BBN time,
  - $n_\rho$: the dark energy density decrease exponent,
  - $\kappa_s$: the ratio of dark entropy density over radiation entropy density at BBN time,
  - $n_s$: the dark entropy density decrease exponent,

  and the optional arguments
  - $T_\rho$: the temperature in $GeV$ below which the dark energy density is set to 0,
  - $T_s$: the temperature in $GeV$ below which the dark entropy density is set to 0;

- **alter_reheating.x**, which computes the abundance of the elements in cosmological scenarios with modified expansion rates and entropy contents, with the addition of entropy production. The required arguments are
  - $\kappa_\rho$: the ratio of dark energy density over radiation energy density at BBN time,
  - $n_\rho$: the dark energy density decrease exponent,
  - $\kappa_\Sigma$: the ratio of dark entropy production over radiation entropy production at BBN time,
  - $n_\Sigma$: the dark entropy production exponent,
  - $T_r$: the temperature in $GeV$ below which the dark energy density and the entropy production are set to 0.

The different parameters concerning the non-standard cosmological scenarios above will be discussed in more detail in section 2.1.

Some changes to the original code, regarding its layout, were made prior to my work. I have built on this modified version and made some further changes to the layout, in addition to an update of the nuclear reactions and the inclusion of new physics.

## 2.1 Structure of the Original Code

A basic, general description of the BBN physics was given in section 1.1. We will now extend the discussion to include all the relevant equations needed to compute the light element abundances, and how they are implemented in *AlterBBN*. Modifications and extensions to the latest version of the program will be discussed in section 2.2. This review is a more detailed version of that found in the *AlterBBN* manual [42]. New physics that I have implemented in the program will be discussed in chapter 3. Notice that in general expressions or definitions I try to use the standard notation of the temperature, where $T$ is in units of Kelvin, whereas in expressions specific for, or important for the code itself I use the dimensionless variable

$$T_9 = \frac{T}{10^9\ K}\ . \tag{2.1}$$

### 2.1.1 Standard Big Bang Nucleosynthesis

**Nuclear Reactions**

In the original code, all the implemented nuclear reactions have evolution equations on the form

$$N_i\ {}^{A_i}Z_i + N_j\ {}^{A_j}Z_j \longleftrightarrow N_k\ {}^{A_k}Z_k + N_l\ {}^{A_l}Z_l, \tag{2.2}$$

where $A_i \geq A_j$, $A_l \geq A_k$, and the exothermic direction is from left to right. The abundance change of a nuclide $i$ is given by the sum over all forward and reverse reactions involving nuclide $i$, that is

$$\frac{dY_i}{dt} = \sum_{j,k,l} N_i \left( -\frac{Y_i^{N_i} Y_j^{N_j}}{N_i! N_j!} \Gamma_{ij\to kl} + \frac{Y_l^{N_l} Y_k^{N_k}}{N_l! N_k!} \Gamma_{kl\to ij} \right). \tag{2.3}$$

Here, the nuclide abundance is defined as $Y_i = X_i/A_i$, where $X_i = n_i/n_B$ is the mass fraction in nuclide $i$ and $A_i$ its atomic number. $N_i$ is the number of nuclides $i$, $\Gamma_{ij\to kl}$ is the forward reaction rate and $\Gamma_{kl\to ij}$ is the reverse rate (see appendix A for a brief review of the theory regarding the reaction rates). The numerical implementation of this equation is thoroughly explained in both [43] and [46] and will not be further discussed here.

The program tracks the evolution of 26 nuclides from an initial temperature $T_{9,i}$ to a final temperature $T_{9,f}$. Following the numbering of *AlterBBN*, the nuclides that are a part of the code are

- 1: $n$
- 2: $p$
- 3: $^2H$
- 4: $^3H$
- 5: $^3He$
- 6: $^4He$
- 7: $^6Li$
- 8: $^7Li$
- 9: $^7Be$
- 10: $^8Li$
- 11: $^8B$
- 12: $^9Be$
- 13: $^{10}B$
- 14: $^{11}B$
- 15: $^{11}C$
- 16: $^{12}B$
- 17: $^{12}C$
- 18: $^{12}N$
- 19: $^{13}C$
- 20: $^{13}N$
- 21: $^{14}C$
- 22: $^{14}N$
- 23: $^{14}O$
- 24: $^{15}N$
- 25: $^{15}O$
- 26: $^{16}O$

Due to the mass-8 bottleneck explained in chapter 1, insignificant amounts of metals heavier than $^9Be$ were created in the Big Bang Nucleosynthesis. However, although the relic abundances of the heavier elements are negligible even compared to that of $^6Li$ ($^6Li/H \sim 10^{-14}$), some reactions involving carbon, nitrogen, oxygen etc. will break the bottleneck and influence BBN through sub-sequent reactions with the lighter elements. Including more reactions is important to rule out a nuclear fix to the lithium problem (see chapter 1.2.4) and provides an overall better accuracy of the code.

**Iteration Variables**

The program time-evolves the photon temperature $T_9$, the electron chemical potential $\mu_e$ parameterized through the degeneracy parameter $\phi_e \equiv \mu_e/k_B T$, and the quantity $h_\eta$ [43][44][47]. The latter is a lowest order parametric representation of the baryon density (see equations 2.19 and 2.20 with discussion), used for convenience as it is proportional to $\eta$ and remains fairly constant as the universe expands, under the assumption of adiabatic expansion. It is time-evolved from an initial value given by (initial value is here denoted by $i$ and is not to be confused with the nuclide number $i$ in equations 2.2 and 2.3)

$$h_{\eta,i} = M_u \frac{n_{b,i}}{T_{9,i}^3} = M_u \frac{n_{\gamma,i}}{T_{9,i}^3} \eta_i \approx 33685.519 \cdot \eta_0 \left( 1 + \frac{s_{e^\pm}(T_i)}{s_\gamma(T_i)} \right) \tag{2.4}$$

where $M_u$ is the atomic mass unit and $\eta_0$ the late-time (CMB measured) value of the baryon-to-photon ratio. The relation between the initial and late-time value of $\eta$ is found from equation 1.36 through entropy conservation. In the original code the initial ratio between the entropy of the electrons/positrons and the photons is approximated to 7/4, assuming $m_e \to 0$. Since the $e^\pm$-pairs are not fully relativistic this imposes a small error in $h_{\eta,i}$. At $T = 2$ MeV Nollett & Steigman [48] estimate that an accurate treatment of the $e^\pm$ entropy gives $s_{e^\pm}$ a value about 2% below its relativistic approximation. In the updated *AlterBBN* the assumption of $m_e \to 0$ is relaxed, leading to a more accurate initial estimate of

$h_\eta$. This modification of the original code is further discussed in section 2.2.5. In the last equality in equation 2.4 I have inserted the physical constants to reveal the *AlterBBN*-implemented expression, which is in units of $g\ cm^{-3}\ K^{-3}$. I will also do so in some other cases later, and this is done to clarify the origin of some of the numerical factors that the reader may encounter if consulting the program code.

$T_9$, $\phi_e$ and $h_\eta$ are used to find the density and pressure of the relevant particles, described in the following. First, the equation of energy conservation may be written as

$$\frac{d}{dt}(\rho_{\text{tot}}a^3) + P_{\text{tot}}\frac{d}{dt}(a^3) - a^3\frac{d\rho_{\text{tot}}}{dt}\bigg|_{T=const} = 0\,, \tag{2.5}$$

from which we may obtain [44]

$$\frac{dr}{dT_9} = -\frac{\frac{d\rho_{\text{tot}}}{dT_9}}{\rho_{\text{tot}} + \frac{P_{\text{tot}}}{c^2} + \left(\frac{1}{dr/dt}\right)\frac{d\rho_{\text{tot}}}{dt}\Big|_{T_9}}\,, \tag{2.6}$$

where $r \equiv ln(a^3)$, which incorporates the thermodynamic effect of the universal expansion on the particle temperatures. If we assume that the neutrinos have already decoupled the total energy density and pressure is given by

$$\rho_{\text{tot}} = \rho_\gamma + \rho_b + (\rho_{e^-} + \rho_{e^+})\,, \tag{2.7}$$

and

$$P_{\text{tot}} = P_\gamma + P_b + (P_{e^-} + P_{e^+})\,. \tag{2.8}$$

This is needed to find the time-derivatives of the temperature:

$$\frac{dT_9}{dt} = \frac{dr/dt}{dr/dT_9}\,, \tag{2.9}$$

and the electron degeneracy parameter:

$$\frac{d\phi_e}{dt} = \frac{\partial\phi_e}{\partial T_9}\frac{dT_9}{dt} + \frac{\partial\phi_e}{\partial r}\frac{dr}{dt} + \frac{\partial\phi_e}{\partial S}\frac{dS}{dt}, \tag{2.10}$$

where $S = \sum_i Z_i Y_i$, $Z_i$ being the charge number of nuclei $i$. The numerical implementation of this expression requires a detailed review of the different derivatives, which will not be given here. Instead, I refer to appendix D in *Kawano 1992* [44] where all relevant information can be found. The time derivative of $h_\eta$ is found by the reasoning that $h_\eta \sim \rho_b/T^3 \sim 1/a^3/T^3$ (see equation 2.19 with discussion), that is

$$\frac{dh_\eta}{dt} = -3h_\eta\left(\frac{1}{a}\frac{da}{dt} + \frac{1}{T_9}\frac{dT_9}{dt}\right)\,. \tag{2.11}$$

The energy density of the photons is given by the bosonic part of equation 1.19, thus

$$\rho_\gamma = \frac{1}{c^2}\frac{g_\gamma\pi^2}{30}\frac{(k_B T)^4}{(\hbar c)^3} = 8.41828\cdot T_9^4\,, \tag{2.12}$$

since $g_\gamma = 2$. The last equality is how it is implemented in *AlterBBN*, and is in units of $g\ cm^{-3}$. The pressure is related to the density by

$$\frac{P_\gamma}{c^2} = \frac{1}{3}\rho_\gamma. \tag{2.13}$$

In the case that the neutrino asymmetry is zero, the energy density of the neutrinos is given by the fermionic part of equation 1.19, yielding

$$\rho_\nu = \frac{1}{c^2}g_\nu N_{\text{eff}}\frac{7}{8}\frac{\pi^2}{30}\frac{(k_B T_\nu)^4}{(\hbar c)^3} = 12.79384\left[g_\nu N_{\text{eff}}\frac{\pi^2}{30}T_{9,\nu}^4\right]\,, \tag{2.14}$$

given in units of $g\ cm^{-3}$. For the SBBN scenario $g_\nu = 2$ and $N_{\text{eff}} = 3$ or, if relaxing the assumptions of instantaneous neutrino decoupling and extremely relativistic $e^\pm$ pairs, $N_{\text{eff}} = 3.046$, as explained in chapter 1.1. Any neutrino degeneracy will lead to a non-zero chemical potential and a bit more involved evaluation of the expression in the square brackets, which will be discussed in section 2.1.2. The neutrino temperature is found by the assumption that the baryon number is conserved, such that $n_b a^3 = constant$, combined with the requirement that the neutrinos simply redshift with the expansion of the universe, leading to

$$T_{\nu 9} = T_{9,i} \left( \frac{h_\eta T_9^3}{\rho_{b,0}} \right)^{1/3} . \tag{2.15}$$

Note that the assumption that $T_\nu \propto a^{-1}$ is true only in the standard scenario. In the presence of e.g. a neutrino coupled WIMP the neutrinos will be heated relative to the photons as the WIMP annihilates, and equation 2.15 is no longer valid. This will be further discussed in chapter 3.

Since the assumption of extremely relativistic electrons and positrons is not entirely accurate at the time of BBN, one cannot simplify the expressions 1.15, 1.16 and 1.17 the same way as was done to find the photon and neutrino densities. Inspired by the method described by Wagoner [43] and the Kawano code [44] the expressions are approximated by using the modified Bessel functions of second type through the definitions

$$L(z) = \frac{K_2(z)}{z}, \qquad M(z) = \frac{1}{z}\left[\frac{3}{4}K_3(z) + \frac{1}{4}K_1(z)\right], \qquad N(z) = \frac{1}{z}\left[\frac{1}{2}K_4(z) + \frac{1}{2}K_2(z)\right] , \tag{2.16}$$

where $z = m_e c^2/k_B T$ and $K_\alpha$ are the modified Bessel function of order $\alpha$. Using these approximations the expressions for the sum of the electron/positron densities and pressures then reads (see appendix C for derivation)

$$\rho_{e^-} + \rho_{e^+} = \frac{1}{c^2}\frac{g_e}{\pi^2}\frac{(m_e c^2)^4}{(\hbar c)^3}\sum_{n=1}^{\infty}(-1)^{n+1}\cosh(n\phi_e)M(nz) \tag{2.17}$$

$$\frac{P_{e^-} + P_{e^+}}{c^2} = \frac{1}{c^2}\frac{g_e}{\pi^2}\frac{(m_e c^2)^4}{(\hbar c)^3}\sum_{n=1}^{\infty}\frac{(-1)^{n+1}}{nz}\cosh(n\phi_e)L(nz) \tag{2.18}$$

Using that $g_e = 2$ and that $m_e c^2 = 0.51100$ MeV $= 8.18700 \cdot 10^{-7}$ erg $= 8.18700 \cdot 10^{-7}\ g\ cm^2\ s^{-2}$ (electrons and positrons), the pre-factor is equal to $3205.724\ g\ cm^{-3}$. Note that the electron and positron chemical potentials have the opposite sign, thus $\phi_e = \phi_{e^-} = -\phi_{e^+}$. The expressions 2.16 are further used to approximate the derivatives of these quantities, among others, needed to compute equations 2.11, 2.9 and 2.10.

**Baryon Density Derivative**

The baryon density is given by the first order approximation (from equation 2.4)

$$\rho_b \approx h T_9^3. \tag{2.19}$$

This approximation is, however, not accurate enough when calculating the derivative of the baryon density, which would drop out of equation 2.6. Including higher order terms, Wagoner [43] describes a more complete expression for the baryon density, given by

$$\begin{aligned}\rho_b &= n_b \left[ M_u + \sum_i \left( \Delta M_i + \frac{3k_b T}{2c^2} \right) Y_i \right] \\ &= h_\eta T_9^3 \left[ 1 + \sum_i \left( \frac{\Delta M_i}{M_u} + \zeta T_9 \right) Y_i \right] ,\end{aligned} \tag{2.20}$$

where $\Delta M_i$ is the mass excess [2] of nuclide $i$ and $\zeta = 1.388 \cdot 10^{-4}$. The non-zero part of the temperature-derivative of the baryon energy density is then

$$\frac{d\rho_b}{dT_9} = h_\eta T_9^3 \zeta \sum_i Y_i \ , \tag{2.21}$$

while the baryon pressure is given by [44]

$$P_b = h_\eta T_9^3 \left( \frac{2}{3} \zeta T_9 \sum_i Y_i \right) . \tag{2.22}$$

**Charged Lepton Degeneracy**

The charged lepton ($e^\pm$) degeneracy will depend on the electron chemical potential, which is parameterized through $\phi_e$. Like in the case with the electron and positron density and pressure, their number densities are approximated through the modified Bessel functions (from equation 1.15), and the expression for their difference reads

$$n_{e^-} - n_{e^+} = \frac{g_e}{\pi^2} \left[ \frac{m_e c^2}{\hbar c} \right]^3 \sum_{n=1}^{\infty} (-1)^{n+1} \sinh(n\phi_e) L(nz) \ . \tag{2.23}$$

This can also be found by charge conservation, which gives

$$n_{e^-} - n_{e^+} = \mathcal{N}_A h_\eta T_9^3 S, \tag{2.24}$$

where $\mathcal{N}_A$ is the Avogadro number, which by definition is $\mathcal{N}_A = 1/M_u$. Charge conservation limits the charged lepton asymmetry to be of the same order as the baryon asymmetry, meaning that $\mu_e / k_B T \sim 10^{-9}$ prior to $e^\pm$ annihilation, which is illustrated in figure 2.1. By equating the two expressions for the difference between the number densities of electrons and positrons, using that $\sinh(x) \approx x$ for $x \ll 1$ and inserting the dimensionless variable $z = m_e c^2 / k_B T$, we find for the initial value of $\phi_e$:

$$\begin{aligned} \phi_e(T_{9,i}) &\approx \frac{\pi^2}{2} \frac{(k_B \hbar c)^3}{M_u} \frac{h_\eta(T_{9,i}) Y_{p,i}}{(10^9 z_i)^3} \frac{1}{\sum_{n=1}^{\infty} (-1)^{n+1} n L(n z_i)} \\ &\approx 3.568 \cdot 10^{-5} \cdot \frac{h_\eta(T_{9,i}) Y_{p,i}}{z_i^3 \sum_{n=1}^{\infty} (-1)^{n+1} n L(n z_i)} \ , \end{aligned} \tag{2.25}$$

where the subscript $i$ means initial value, and we have used that prior to BBN the baryon budget consisted of only protons and neutrons, thus

$$\sum_i Z_i Y_i = Z_n Y_n + Z_p Y_p = 0 \cdot Y_n + 1 \cdot Y_p = Y_p . \tag{2.26}$$

**Initial Abundances**

The initial abundances of protons and neutrons are described by the distribution functions

$$Y_p(T_i) = \frac{1}{1 + e^{-Q/T_i}} \ , \qquad Y_n(T_i) = \frac{1}{1 + e^{Q/T_i}} \ , \tag{2.27}$$

where $Q$ is the difference between the neutron and proton masses, which was encountered in equation 1.38. These values are thus naturally dependent on the neutron-to-proton ratio at temperature $T_i$. The initial time is found by (approximation for $T \to \infty$ and $t \to 0$ [47])

$$t_i = (12\pi G \sigma c^{-2})^{1/2} T_{9,i}^{-2} \approx (0.09615 \cdot T_{9,i})^{-2} , \tag{2.28}$$

where $\sigma$ is Stefan-Boltzmann's constant and $G$ is Newton's gravitational constant.

[2] The difference between the actual mass of the nuclide and its mass number in atomic mass units.

### 2.1.2 Modified Cosmological Scenarios

Several unknown physical processes may influence the evolution of the early universe. *AlterBBN* has the options of modifying the number of neutrino families and impose a neutrino degeneracy among the standard model neutrinos, in addition to modifying the expansion rate and entropy content directly. Moreover, it can apply reheating models with a resulting entropy production. These modified cosmological scenarios influence the properties of the early universe in different ways, and in the following we will explain the physics and how they are implemented in the program. In this discussion I will set $k_B = \hbar = c = 1$.

**Adding equivalent neutrinos and a Non-Zero Neutrino Degeneracy**

Adding equivalent neutrinos alone has the effect of speeding up the expansion of the universe through an increased energy density. The extra radiation is absorbed into the neutrino energy density, given by equation 2.14, through the definition of $N_{\text{eff}}$ (see chapter 1.1.6). Using a non-zero neutrino degeneracy, on the other hand, will lead to a more involved calculation of the neutrino energy density. In chapter 1.1 we gave a detailed description of the neutrino degeneracy parameter $\xi$ and explained that due to mixing of the standard model neutrinos, one usually assumes that the chemical potential of the three species are equal, thus writing $\xi = \xi_e = \xi_\mu = \xi_\tau$. However, *AlterBBN* gives the user the option to provide differing values of $\xi_e$, $\xi_\mu$ and $\xi_\tau$. We also mentioned that any contribution to the expansion rate ($\mathcal{S} \neq 0$) emerging from a non-zero neutrino degeneracy is very small, and is likely to yield differences in the relic abundances smaller than the observationally imposed uncertainties. Although this may be true we still need to keep track of it, since the combined effect of multiple small modifications to the standard cosmology scenario may lead to significant changes in the abundances. In *AlterBBN* this effect is implemented by modifying the neutrino density to [44]

$$\rho_{\nu_\alpha,\overline{\nu}_\alpha} = \frac{1}{2\pi^2} T_\nu^4 \int_0^\infty dx \frac{x^3}{1+\exp(x \mp \xi_{\nu_\alpha})} , \tag{2.29}$$

where it is assumed that the three species share the same temperature, and the total neutrino density is found by summing over the three neutrino species $\nu_\alpha$, $\alpha = e, \mu, \tau$. The minus sign in the exponential is for the neutrinos and the plus sign is for the anti-neutrinos. Integrating this expression is quite time consuming, so that in the case of a very small neutrino degeneracy ($\xi \leq 0.03$) the approximation [44]

$$\rho_{\nu_\alpha} + \rho_{\overline{\nu}_\alpha} = \frac{\pi^2}{15} T_\nu^4 \left( \frac{7}{8} + \frac{15}{4\pi^2}\xi_{\nu_\alpha}^2 + \frac{15}{8\pi^4}\xi_{\nu_\alpha}^4 \right) \tag{2.30}$$

is used, while the approximation [44]

$$\rho_{\nu_\alpha} + \rho_{\overline{\nu}_\alpha} = \frac{1}{8\pi^2}(T_\nu \xi_\nu)^4 \left[ 1 + \left( \frac{2\pi^2}{\xi_\nu^2} \right) \right] \tag{2.31}$$

is used for very large values ($\xi \geq 30$). For $0.03 < \xi < 30$ equation 2.29 must be integrated numerically.

The most important effect of a non-zero neutrino degeneracy is the altered neutron-to-proton ratio through charged current weak interactions involving the electron neutrinos and anti-neutrinos. This leads to a modification of the weak rates controlling the $p \leftrightarrow n$ reaction, and the initial abundances of protons and neutrons are changed from the ones given in 2.27 to

$$Y_p(T_i) = \frac{1}{1+e^{-Q/T_i - \xi_{\nu e}}} , \qquad Y_n(T_i) = \frac{1}{1+e^{Q/T_i + \xi_{\nu e}}} . \tag{2.32}$$

**Modified Expansion Rate**

Contributions to the total relativistic energy at the time of BBN will change the expansion rate of the universe and consequently the primordial abundances. In *AlterBBN* one can parameterize any such

phenomena by adding an effective dark energy density $\rho_D$ to the first Friedmann equation, which is then modified from equation 1.6 ($k = 0$) to

$$H^2 = \frac{8\pi G}{3}(\rho_{\text{tot}} + \rho_D) \, . \tag{2.33}$$

As a parameterization for $\rho_D$ the code adopts, as described in [49] [50],

$$\rho_D = \kappa_\rho \rho_{\text{tot}}(T_0) \left(\frac{T}{T_0}\right)^{n_\rho} \, , \tag{2.34}$$

where $k_B T_0 = 1$ MeV. $\kappa_\rho$ is then the ratio of effective dark density over the total energy density, and $n_\rho = 3(1 + w)$ is a constant parameterizing the density behavior, depending on whether it behaves like radiation ($n_\rho = 4$), matter ($n_\rho = 3$), vacuum energy ($n_\rho = 6$) etc. (see chapter 1.1.2 for the definition of $w$, and [49] for more information about $n_\rho$).

**Modified Entropy Content**

The entropy content can also receive various contributions from unknown sources, e.g. from exotic particles that annihilate during BBN and heats the photons relative to the neutrinos or vice versa. In the original code any such contribution is parameterized in a generic way by considering an effective dark entropy density $s_D$, so that the energy conservation is modified from equation 2.5 to

$$\frac{d}{dt}(\rho_{\text{tot}} a^3) + P_{\text{tot}} \frac{d}{dt}(a^3) - a^3 \frac{d\rho_{\text{tot}}}{dt}\bigg|_{T=const} - T \frac{d}{dt}(s_D a^3) = 0 \, . \tag{2.35}$$

In the case of no reheating, the parameterization (described in [50])

$$s_D = \kappa_s s_{\text{rad}}(T_0) \left(\frac{T}{T_0}\right)^{n_s} \tag{2.36}$$

is used, where $k_B T_0 = 1$ MeV, and

$$s_{\text{rad}}(T) = h_{\text{eff}}(T) \frac{2\pi^2}{45} T^3 \, , \tag{2.37}$$

$h_{\text{eff}}$ being the effective number of entropic degrees of freedom of radiation, $\kappa_s$ the ratio of effective dark entropy density over radiation entropy density, and $n_s$ a constant parameterizing the entropy behavior, depending on whether it is radiation-like, matter-like etc. (see [50] for specific values of this). In the case that a particle annihilates and reheats the plasma, however, there will be additional entropy production. Arbey et al. [51] describes an evolution of the entropy production $\Sigma_D$ according to

$$\Sigma_D(T) = \kappa_\Sigma \Sigma_{\text{rad}}(T_0) \left(\frac{T}{T_0}\right)^{n_\Sigma} \, , \tag{2.38}$$

where again $k_B T_0 = 1$ MeV. $\kappa_\Sigma$ is the ratio of effective dark entropy production over radiation entropy production while $n_\Sigma$ describes the behavior of the entropy production, which in most reheating scenarios will be $n_\Sigma \sim -1$ (see [51]). The radiation entropy production reads:

$$\Sigma_{\text{rad}}(T_0) = \left(\frac{4\pi^3 G}{5} g_{\text{eff}}(T_0)\right)^{1/2} T_0^2 s_{\text{rad}}(T_0) \, , \tag{2.39}$$

$g_{\text{eff}}$ being the effective number of degrees of freedom of radiation. The dark entropy density is then found by integrating over the entropy production, as

$$s_D(T) = 3\sqrt{\frac{5}{4\pi^3 G}} h_{\text{eff}} T^3 \int_0^T dT' \frac{g_*^{1/2} \Sigma_D(T')}{\sqrt{1 + \frac{\rho_D}{\rho_{\text{rad}}}} h_{\text{eff}}^2(T') T'^6} \, , \tag{2.40}$$

where

$$g_*^{1/2} = \frac{h_{\text{eff}}}{\sqrt{g_{\text{eff}}}} \left(1 + \frac{T}{3h_{\text{eff}}} \frac{dh_{\text{eff}}}{dT}\right) \, . \tag{2.41}$$

## 2.2 Changes to The Original Code

The main tasks of this project were to get the nuclear network of *AlterBBN* up to date and to add new physics to the code. However, working with the original code I soon realized that I had to make some changes to the interface and layout, to facilitate the desired runs and extraction of data. Prior to my work, some changes were made in this regard, and I have built on these modifications plus added some more. In this section I will go through all the changes, up until the inclusion of new physics, which will be discussed in chapter 3. The changes discussed here are

- **New layout/interface**, related to how the program is run. Instead of five main programs for different cosmological scenarios, all the physics is collected into one program, with parameter inputs given in a *.ini*-file. An external *PYTHON* program was made to execute *AlterBBN*. This is very convenient in the case that we want to do multiple runs with *AlterBBN*, varying parameters like the baryon-to-photon ratio, WIMP mass etc.

- **Correction of the initial time** when including extra relativistic degrees of freedom.

- **Extension of the nuclear network**, with the addition of 12 new reactions to the original 88. The new reactions are implemented as in *PArthENoPE* [45].

- **Updated reaction rates** for six important reactions: $H(n,\gamma)^2H$ [52], $^7Be(n,\alpha)^4He$ [53], $^3He(\alpha,\gamma)^7Be$ [54], $^2H(p,\gamma)^3He$ [55], $^2H(d,n)^3He$ [55] and $^2H(d,p)^3H$ [55].

- **The initial value of the electron-positron entropy density**, needed to estimate the initial value of $h_\eta$, have been corrected to account for the partial non-relativistic nature of the $e^\pm$-pairs around the time of neutrino decoupling.

In addition to these updates, a few bugs were discovered in the original version. The first one involves the array *double reacparam* in the function *nucl* (and *nucl_failsafe*), where the reactions $^{12}N(\alpha,p)^{15}O$ and $^{13}N(\alpha,p)^{16}O$ (reactions number 92 and 93 in the updated version) were of the wrong reaction type. Those have been changed from type 3 to type 2 (see section 2.2.3) in the updated version. A second error was found in the reaction rate of the reaction $^3H(D,n)^4He$ (number 30), which originally contained a factor $1.8764462 \cdot 10^9 T_9^2$. According to *Serpico et al.* [56] this should be $1.8764462 \cdot 10^9 T_9^3$, and has been changed accordingly in the updated version. Finally, the contribution from thermally excited levels to the reaction $^{13}C(p,\gamma)^{14}N$, which is reaction number 73 in the updated version, was wrongly added to reaction number 72 instead. This has now been corrected.

### 2.2.1 New Layout/Interface

As discussed in the introduction to this chapter, the original code consists of five main programs concerning different cosmological scenarios. Except from the program computing the parameter-free standard cosmological model, using the CMB-measured value of $\eta$, they all require a various number of input arguments. For the two programs involving dark energy/dark entropy density and entropy production, the number of input arguments is quite large (4-6), and having to enter all those arguments for every run can be a source of frustration. As mentioned, a modification to this layout was made prior to my work, by Digvijay Wadekar at the University of Oslo [57]. The five main programs were compressed into two; the first one covering *stand_cosmo*, *alter_eta* and *alter_neutrinos*, requiring the parameters to be given in a separate *.ini*-file (named *input.ini*); the second one covering *alter_standmod* and *alter_reheating*, requiring the parameters to be given in the code itself. I find it convenient to collect all parameters that can be changed by the user in one single file, even though some of them may not be used as much as

others. I also combined the two programs into one, making it more practical both to work with and to use, even though the *main*-part of the code got a bit more involved. The addition of WIMPs (see chapter 3) was also implemented into this new, combined program. The new layout thus consists of only one main code, *primary.c*, using the input file *input.ini* to extract parameter values given by the user.

To differ between the various cosmological models, the executable *primary.x* now takes one input argument. If this argument is **standard** the program will collect the parameters $\eta$, $\tau$, $N_\nu$, $\Delta N_\nu$, $\xi_{\nu_e}$, $\xi_{\nu_\mu}$ and $\xi_{\nu_\tau}$ from the input file, and use those in the computation. Although not a part of *standard* cosmology, I decided to include the neutrino degeneracy parameters in this option to minimize the number of input argument options. If the user do not want to include any neutrino degeneracy, these parameters must therefore be set to zero. Using the argument **darkdens** together with the executable will modify the expansion rate and entropy content, and concerns the parameters $\kappa_\rho$, $n_\rho$, $\kappa_s$, $n_s$, $T_\rho$ and $T_s$, while the argument **reheating** will modify the expansion rate and add entropy production, thus concerning the parameters $\kappa_\rho$, $n_\rho$, $\kappa_\Sigma$, $n_\Sigma$ and $T_r$. By default, the different cut-off temperatures are set to 0, which means that the program will take equations 2.34, 2.36 and 2.40 into consideration throughout the whole run, but the user is free to change these parameters through the input file. To invoke simulations including WIMPs the user may give the argument **wimp**. The parameters that need to be set through the input file in this setting is the WIMP mass, the type of WIMP, its coupling to the standard model particles, and its chemical potential. Further details of these parameters will be given in chapter 3. Finally, the user may run the executable without giving any arguments. The program will then run the parameter-free standard cosmology scenario with $\eta_{10} = 6.10$, $\tau = 880.3$ and $N_{eff} = N_\nu = 3.046$. Note that for the options **darkdens** and **reheating** the parameters $\eta$, $\tau$, $N_\nu$, $\Delta N_\nu$, $\xi_{\nu_e}$, $\xi_{\nu_\mu}$ and $\xi_{\nu_\tau}$ are also set through the *.ini*-file. A combination of the options **darkdens**, **reheating** and **wimp** is possible, since there might exist interesting cases where e.g. a light WIMP with specified properties is combined with extra radiation/entropy of an unspecified nature. Beware that with this combination implemented, it is essential that all parameters controlling the **darkdens** and **reheating** options are set to zero when a "combination-less" WIMP run is made. For all individual options (**standard**, **darkdens** and **reheating**), on the other hand, none of the parameters that are not part of the option are included in the calculation.

*AlterBBN* does not come with the functionality of internally varying any of the parameters that go into the computation. Such an option is necessary if we want to study the change in the resulting abundances by varying e.g. the baryon-to-photon ratio. Instead of modifying the program itself to do this, I wrote an external *PYTHON* program for compiling and executing *AlterBBN*, which I have called *ARES*. This interacts with the input file, and enables the user to run *AlterBBN* for as many times as desired while varying a parameter of choice. The parameters that are allowed to vary is the baryon-to-photon ratio ($\eta$), both the equivalent number of neutrinos ($\Delta N_\nu$) and the effective number of neutrinos ($N_{eff}$) as well as all the neutrino degeneracy parameters ($\xi_e$, $\xi_\mu$ and $\xi_\tau$), the neutron lifetime ($\tau_n$), the WIMP mass ($m_\chi$) and the WIMP electron chemical potential parameterized as a degeneracy parameter ($\phi_\chi$). A switch may be used to show a plot of the light element abundances of $D$, $^4He$, $^3He$ and $^7Li$ as a function of $\eta$ if this is chosen as the free parameter (see figure 1.4). The results from all the runs are written to the file *alterdata.txt*, which may then be used to make plots etc.

The program may also be used in the case that all parameters are fixed (single *AlterBBN* run). This way the user do not have to compile *AlterBBN* before running, rather just execute *ARES*. Also, a switch to direct the results from the terminal to the output-file *alterdata.txt* is included, in the case that the user want to use those after running *AlterBBN* in the fixed parameter case.

*ARES* is executed by giving a minimum of two input arguments; the first one determining the type of run (**single** or **multi**); the second one determining the type of cosmology (**paramfree**, **standard**, **darkdens**, **reheating** or **wimp**). The **paramfree** option is equivalent to running *AlterBBN* with no input argument, using the parameter-free SBBN scenario with $\eta_{10} = 6.10$, $\tau_n = 880.3$ and $N_{eff} = N_\nu = 3.046$. The other options are thoroughly explained in the above discussion. The default settings are $\eta$ as the parameter to vary, with 25 values between the limits $\eta_{min} = 10^{-10}$ and $\eta_{max} = 10^{-9}$, as well as a log distribution of the 25 points. The default settings may be temporarily changed by providing further input

arguments. For an explanation of all the possible options, the program may be run with the one input argument **info**.

### 2.2.2 Correction of the Initial Time

The initial time for the BBN calculation is given by equation 2.28. However, this approximation is true only in the standard scenario. The original code includes the option of adding extra relativistic degrees of freedom to the mix, in the form of an unspecified "dark density". A positive value of the dark density will contribute to an increased expansion rate, leading to less elapsed time for a given temperature than in the SBBN scenario. It will not affect the abundances, since the dynamic variables $T_9$, $h_\eta$ and $\phi_e$ only depends on the time-steps and not the absolute time at where they are analyzed. However, there are situations where we would want to keep track of the cosmic time. For example, in chapter 3 we plot the time evolution of the photon temperature for standard and WIMP scenarios, where it is essential to know the initial time.

The correction is based on the assumption that for high temperatures the expansion rate is inversely proportional to the time, or $H \propto t^{-1}$. This is a valid assumption at the high temperatures for our purposes, knowing that it will not impose uncertainties on the light element abundances. The new initial time is then given by

$$t_{\text{new}} = t_{\text{SBBN}} \frac{H_{\text{SBBN}}}{H_{\text{new}}} \,, \tag{2.42}$$

where $t_{\text{SBBN}}$ is given by equation 2.28. Note that *AlterBBN* does not assume $H \propto t^{-1}$ when calculating the expansion rate, since this is not entirely true, and would impose uncertainties on the calculation of the relic abundances of the light elements. Thus $H_{\text{SBBN}}$ is given by the energy densities of photons, neutrinos, $e^{\pm}$-pairs and baryons, while $H_{\text{new}}$ also includes the dark density. In case that we (also) want to include WIMPs, there will be an (additional) correction factor for their contribution to the total energy density at the starting time (see chapter 3).

### 2.2.3 Extension of the Nuclear Network

In table 2.6 I have listed the full nuclear network of *AlterBBN*, including the new reactions, (marked by an asterisk). The change in the element abundances from extending the nuclear network can be seen in table 2.1, where the results are obtained from SBBN runs. We see that extending the nuclear network has a very small effect on the abundances. The largest differences are found in the estimates of $D$ and $^6Li$, but we also note that the uncertainties in these two predictions have increased.

The nuclear network in the original code only consists of reactions on the form 2.2, and is not generalized to the case of three-body reactions including three different nuclides. Amongst the new reactions added to the program is

$$^3He + {}^3H \longleftrightarrow n + p + {}^4He \,, \tag{2.43}$$

which includes three different nuclides on the right side. The code therefore had to be modified along the same lines as *NUC123* and *PArthENoPE* to cover this type of reaction as well. All reactions are now on the form

$$N_i \, {}^{A_i}Z_i + N_j \, {}^{A_j}Z_j + N_g \, {}^{A_g}Z_g \longleftrightarrow N_h \, {}^{A_h}Z_h + N_k \, {}^{A_k}Z_k + N_l \, {}^{A_l}Z_l \,, \tag{2.44}$$

and this leads to a simple extension of equation 2.3, which now reads

$$\frac{dY_i}{dt} = \sum_{j,g,h,k,l} N_i \left( -\frac{Y_i^{N_i} Y_j^{N_j} Y_g^{N_g}}{N_i! N_j! N_g!} \Gamma_{ijg \to hkl} + \frac{Y_h^{N_h} Y_k^{N_k} Y_l^{N_l}}{N_h! N_k! N_l!} \Gamma_{hkl \to ijg} \right) . \tag{2.45}$$

| | Org. code | Ext. network |
|---|---|---|
| $Y_p$ * | 0.2472 | 0.2471 |
| $\Delta Y_p$ † | - | -0.04 |
| $\delta Y_p$ ‡ | 0.045 | 0.045 |
| $[D/H]_p \times 10^5$ | 2.5730 | 2.5780 |
| $\Delta[D/H]_p$ | - | 0.19 |
| $\delta[D/H]_p$ | 1.40 | 1.56 |
| $[^3He/H]_p \times 10^5$ | 1.0240 | 1.0250 |
| $\Delta[^3He/H]_p$ | - | 0.10 |
| $\delta[^3He/H]_p$ | 4.29 | 3.55 |
| $[^7Li/H]_p \times 10^9$ | 0.4567 | 0.4546 |
| $\Delta[^7Li/H]_p$ | - | -0.46 |
| $\delta[^7Li/H]_p$ | 7.14 | 5.93 |
| $[^6Li/H]_p \times 10^{14}$ | 1.1220 | 1.1350 |
| $\Delta[^6Li/H]_p$ | - | 1.16 |
| $\delta[^6Li/H]_p$ | 87.02 | 91.19 |
| $[^7Be/H]_p \times 10^9$ | 0.4290 | 0.4269 |
| $\Delta[^7Be/H]_p$ | - | -0.49 |
| $\delta[^7Be/H]_p$ | 7.25 | 5.93 |

*Table 2.1: The resulting abundances for two different AlterBBN runs. The first run was made with the original code, while the results from extending the nuclear network from 88 to 100 reactions are shown in the rightmost column. Both runs were made assuming SBBN, with* $\eta_{10} = 6.10$*,* $N_\nu = 3.046$ *and* $\tau_n = 880.3$*.*
** Central abundance value.*
*† Change in the abundance relative to the run made with the original code, given in percent.*
*‡ Linearly calculated abundance uncertainty, relative to the central abundance, given in percent.*

Extending the program to be able to handle reactions on the form 2.43 involved modifying the function *int linearize* found in the routine *bbn.c*. In appendix A we discuss the relevant theory for making the extension from four to six nuclides. In table 2.2 I have listed the different reaction types found in the updated version of *AlterBBN*, together with the corresponding equations for finding $\Gamma_{ijg\to hkl}$ (equation A.11) and $\Gamma_{hkl\to ijg}$ (equation A.12). I have also given the values of the variables CN1, CN2, CN3, CN4, CN5 and CN6, which are needed in the numerical integration of equation 2.45. This involves building a matrix equation for the abundance changes, and the relevant steps in solving this matrix equation are given in [44]. A detailed discussion of this is beyond the scope of this project, but since we need the values of CN1-CN6 for the new type of reaction, I will briefly explain this step from the numerical recipe. By comparing equation E.7 in [44] with the method used in *PArthENoPE* (which is the same method as the one used in *AlterBBN*, except that in *PArthENoPE* the variables are written out in their full form), we find that

$$CN1 = \frac{N_i Y_i^{N_i-1} Y_j^{N_j} Y_g^{N_g}}{(N_i + N_j + N_g) N_i! N_j! N_g!} \Gamma_{ijg\to hkl} \ . \tag{2.46}$$

For CN2 and CN3 we have the same expression, only we switch $i$ with $j$ and $i$ with $g$ respectively. Likewise, we get

$$CN4 = \frac{N_h Y_h^{N_h-1} Y_k^{N_k} Y_l^{N_l}}{(N_h + N_k + N_l) N_h! N_k! N_l!} \Gamma_{hkl\to ijg} \ , \tag{2.47}$$

and we similarly switch $h$ with $k$ and $h$ with $l$ to find CN5 and CN6 respectively.

The energy output $Q$, and the reverse reaction coefficient $C_{\text{rev}}$ are calculated externally and put into the matrix *double reacparam*, which is defined in the function *nucl* (and *nucl_failsafe*). The energy output from the reaction is simply the difference in excess masses, that is

$$Q = N_i dm_i + N_j dm_j + N_g dm_g - N_h dm_h - N_k dm_k - N_l dm_l \ , \tag{2.48}$$

| Type | $(N_i,N_j,N_g,N_h,N_k,N_l)$ | $\frac{\Gamma_{ijg\to hkl}}{\hat{f}_{ijg}}$ | $\frac{\Gamma_{hkl\to ijg}}{C_{\rm rev}\hat{f}_{ijg}e^{-11.605Q_6/T_9}}$ | $\frac{(CN1,CN2,CN3)}{\Gamma_{ijg\to hkl}}$ | $\frac{(CN4,CN5,CN6)}{\Gamma_{hkl\to ijg}}$ |
|---|---|---|---|---|---|
| 0 | (1,0,0,0,0,1) | - | - | (1,0,0) | (0,0,1) |
| 1 | (1,1,0,0,0,1) | $\rho_b$ | $0.987\cdot10^{10}T_9^{3/2}$ | $(Y_j/2,Y_i/2,0)$ | (0,0,1) |
| 2 | (1,1,0,0,1,1) | $\rho_b$ | $\rho_b$ | $(Y_j/2,Y_i/2,0)$ | $(0,Y_l/2,Y_k/2)$ |
| 3 | (1,0,0,0,0,2) | - | - | (1,0,0) | $(0,0,Y_l/2)$ |
| 4 | (1,1,0,0,0,2) | $\rho_b$ | $\rho_b$ | $(Y_j/2,Y_i/2,0)$ | $(0,0,Y_l/2)$ |
| 5 | (2,0,0,0,1,1) | $\rho_b$ | $\rho_b$ | $(Y_i/2,0,0)$ | $(0,Y_l/2,Y_k/2)$ |
| 6 | (3,0,0,0,0,1) | $\rho_b^2$ | $0.974\cdot10^{20}T_9^3$ | $(Y_i^2/6,0,0)$ | (0,0,1) |
| 7 | (2,1,0,0,0,1) | $\rho_b^2$ | $0.974\cdot10^{20}T_9^3$ | $(Y_jY_i/3,Y_i^2/6,0)$ | (0,0,1) |
| 8 | (1,1,0,0,1,2) | $\rho_b$ | $1.013\cdot10^{-10}T_9^{-3/2}\rho_b^2$ | $(Y_j/2,Y_i/2,0)$ | $(0,Y_l^2/6,Y_kY_l/3)$ |
| 9 | (1,1,0,0,0,3) | $\rho_b$ | $1.013\cdot10^{-10}T_9^{-3/2}\rho_b^2$ | $(Y_j/2,Y_i/2,0)$ | $(0,0,Y_l^2/6)$ |
| 10 | (2,0,0,0,2,1) | $\rho_b$ | $1.013\cdot10^{-10}T_9^{-3/2}\rho_b^2$ | $(Y_i/2,0,0)$ | $(0,Y_lY_k/3,Y_k^2/6)$ |
| 11 (new) | (1,1,0,1,1,1) | $\rho_b$ | $1.013\cdot10^{-10}T_9^{-3/2}\rho_b^2$ | $(Y_j/2,Y_i/2,0)$ | $(Y_kY_l/3,Y_hY_l/3,Y_hY_k/3)$ |

*Table 2.2: First column: The 12 different reaction types in the updated* AlterBBN *version. Second column: The number of nuclides involved in each reaction type, according to equation 2.44. Third column: The forward reaction rate used in equation 2.45, given by equation A.11 (divided by the tabulated reaction rate). Fourth column: The reverse reaction rate used in equation 2.45, given by equation A.12 (divided by the tabulated (forward) reaction rate, the reverse reaction coefficient and the exponential in the reverse rate equation, which are all common factors for all reaction types). Fifth column: The three variables CN1, CN2 and CN3 given by equation 2.46 (divided by the forward reaction rate). Sixth column: The three variables CN4, CN5 and CN6 given by equation 2.47 (divided by the reverse reaction rate). The reaction $p\leftrightarrow n$ (type 0) is computed in a separate function in the routine bbnrate.c, which gives $\Gamma$ as output. The rest of the weak reaction rates are independent of temperature and tabulated as constants in the form of $\Gamma$. Hence $\Gamma=\hat{f}$ and we do not have to use equations A.11 and A.12 for reactions of types 0 and 3.*

where $dm_i$ is the excess mass of nuclide $i$. While computing $C_{\rm rev}$ and $Q$ for the new reactions, I did a consistency check on the values used in the original code, and realized that they did not entirely correspond. Doing SBBN runs with both the original and new set of values, varying $\eta$ in the range $[10^{-10},10^{-9}]$, I found a relative difference of up to $\sim 2\%$ for $C_{\rm rev}$ and $\sim 0.2\%$ for $Q$. There might be some discrepancies between some of the input parameters in *AlterBBN* and how they are computed in *PArthENoPE* [58]. In *PArthENoPE*, $C_{\rm rev}$ and $Q$ are calculated inside the program by using equations A.10 and 2.48. It is difficult to explain a $\sim 2\%$ difference in the values of $C_{\rm rev}$ simply by round-offs to a lower precision, thus I suspect that further simplifications of equation A.10 have been made to obtain the values found in *double reacparam* in the original *AlterBBN* code. In table 2.1 I have listed the resulting element abundances for a parameter-free SBBN run, using both the old and the new set of values for $C_{\rm rev}$ and $Q$, only including the original nuclear reaction network. Notice that the change in abundances going from the old set to the new set reach a maximum of 0.5% which is well within the theoretical uncertainties on the reaction rates. However, I do not like to impose unnecessary uncertainties where it could be avoided, so the updated *AlterBBN* will use equation A.10 for the reverse reaction coefficient together with my updated values for the energy output.

### 2.2.4 Updated Nuclear Rates

The task of computing the light element abundances from BBN relies heavily on the nuclear reaction cross sections. In fact, theoretical uncertainties in the abundance predictions are dominated by uncertainties imposed by the nuclear rates, except for the prediction of the $^4He$ abundance, which is dominated by uncertainties in the neutron lifetime and Newton's gravitational constant [59]. In table 2.3 I have listed the leading nuclear reactions in the predictions of the abundances (left table) and the leading nuclear re-

actions in the predictions of the uncertainties (right table) [59]. Most of the reaction rates in the original code regarding these reactions are taken from Serpico et al. 2004 [56], the exceptions being reaction 28 and 29 (Pisanti et al. 2007 [45]).

| Reaction number | Reaction |
|---|---|
| 1 | $p \longleftrightarrow n$ |
| 12 | $p(n,\gamma)D$ |
| 20 | $D(p,\gamma)^3He$ |
| 28 | $D(D,n)^3He$ |
| 29 | $D(D,p)^3H$ |
| 16 | $^3He(n,p)^3H$ |
| 30 | $^3H(D,n)^4He$ |
| 31 | $^3He(D,p)^4He$ |
| 27 | $^3He(\alpha,\gamma)^7Be$ |
| 26 | $^3H(\alpha,\gamma)^7Li$ |
| 17 | $^7Be(n,p)^7Li$ |
| 24 | $^7Li(p,\alpha)^4He$ |

| Reaction number | Reaction |
|---|---|
| 28 | $D(D,n)^3He$ |
| 29 | $D(D,p)^3H$ |
| 20 | $D(p,\gamma)^3He$ |
| 27 | $^3He(\alpha,\gamma)^7Be$ |
| 31 | $^3He(D,p)^4He$ |

*Table 2.3: Left table: The nuclear reactions dominating the predictions of the light element abundances. Right table: The nuclear reactions dominating the prediction of the uncertainties. The reaction number is the number each reaction is given in* AlterBBN*, as presented in table 2.6.*

Recent work by Coc et al. 2015 [55] has provided more precise rates for the deuterium destruction reactions number 20, 28 and 29, which I have added to *AlterBBN*. The article presents tabulated values of the reaction rates for temperatures between 0.001 and 10 $GK$ (see table B.3 in appendix B). For temperatures above 10 $GK$ I set both the reaction rates and the uncertainties to zero, which is a valid assumption for all rates except the weak reaction(s) that transform $p \leftrightarrow n$ [60]. At high temperatures the nuclei disintegrate as soon as they form, that is, they are in nuclear statistical equilibrium. This means that their abundances do not depend on the reaction rates. Of course, there are small deviations from nuclear statistical equilibrium already at temperatures $\sim 10\ GK$. However, since it is difficult to measure rates at such high temperatures we often rely on extrapolations from lower temperatures, which may impose large uncertainties on the estimates. The other extreme is that the program may run below the tabulated temperatures, in which case I have set the rates and uncertainties for reactions number 20, 28 and 29 equal to the values corresponding to the lowest temperatures. However, there is no apparent reason for running *AlterBBN* to temperatures below 0.001 $GK$, since BBN has run its course by then.

New data is also available for reaction rate number 12 through the work of Ando et al. 2004 [52]. This is the reaction that produces deuterium from protons and neutrons and thus a key step in the production of the other light elements. Best-fit formulas for the reaction rate and the corresponding uncertainty are found in appendix B. The authors report a very good agreement between their work and previous theoretical estimations for energies below 0.1 MeV. However, at $E = 0.5$ and $E = 1.0$ MeV they find significant differences from other theoretical estimations they are comparing with, suggesting better experimental measurements of the $n/p$-capture cross sections at these energies before any conclusion can be made. Therefore I use this rate only for $T_9 < 1.5$, which correspond to $\sim 0.13$ MeV. This is right before the deuterium bottleneck is breached, so the new rate will cover the most important stages of BBN. For

| | Org. rates | Rate 12 | Rate 19 | Rate 20 | Rate 27 | Rate 28 | Rate 29 | **All new** |
|---|---|---|---|---|---|---|---|---|
| $Y_p$ * | 0.2471 | 0.2471 | 0.2471 | 0.2471 | 0.2471 | 0.2471 | 0.2472 | **0.2472** |
| $\Delta Y_p$ † | - | 0.00 | 0.00 | 0.00 | 0.00 | 0.00 | 0.04 | **0.04** |
| $\delta Y_p$ ‡ | 0.045 | 0.045 | 0.045 | 0.045 | 0.045 | 0.045 | 0.045 | **0.045** |
| $[D/H]_p \times 10^5$ | 2.5780 | 2.5820 | 2.5780 | 2.5290 | 2.5780 | 2.5500 | 2.5140 | **2.4560** |
| $\Delta[D/H]_p$ | - | 0.16 | 0.00 | -1.90 | 0.00 | -1.09 | -2.48 | **-4.73** |
| $\delta[D/H]_p$ | 1.56 | 1.55 | 1.56 | 1.70 | 1.56 | 1.64 | 1.65 | **2.31** |
| $[^3He/H]_p \times 10^5$ | 1.0250 | 1.0250 | 1.0250 | 1.0440 | 1.0250 | 1.0260 | 1.0090 | **1.0330** |
| $\Delta[^3He/H]_p$ | - | 0.00 | 0.00 | 1.85 | 0.00 | 0.10 | -1.56 | **0.78** |
| $\delta[^3He/H]_p$ | 3.55 | 3.55 | 3.55 | 3.63 | 3.55 | 3.60 | 3.56 | **4.54** |
| $[^7Li/H]_p \times 10^9$ | 0.4546 | 0.4520 | 0.4601 | 0.4712 | 0.5079 | 0.4617 | 0.4576 | **0.5383** |
| $\Delta[^7Li/H]_p$ | - | -0.57 | 1.21 | 3.65 | 11.73 | 1.56 | 0.66 | **18.41** |
| $\delta[^7Li/H]_p$ | 5.93 | 5.95 | 5.84 | 5.95 | 6.22 | 5.89 | 5.88 | **7.53** |
| $[^6Li/H]_p \times 10^{14}$ | 1.1350 | 1.1360 | 1.1350 | 1.1130 | 1.1350 | 1.1230 | 1.1070 | **1.0810** |
| $\Delta[^6Li/H]_p$ | - | 0.09 | 0.00 | -1.94 | 0.00 | -1.06 | -2.47 | **-4.76** |
| $\delta[^6Li/H]_p$ | 91.19 | 91.20 | 91.19 | 91.38 | 91.19 | 91.36 | 91.24 | **86.57** |
| $[^7Be/H]_p \times 10^9$ | 0.4269 | 0.4243 | 0.4322 | 0.4437 | 0.4784 | 0.4342 | 0.4305 | **0.5095** |
| $\Delta[^7Be/H]_p$ | - | -0.61 | 1.24 | 3.94 | 12.06 | 1.71 | 0.84 | **19.35** |
| $\delta[^7Be/H]_p$ | 5.93 | 5.94 | 5.84 | 5.96 | 6.26 | 5.89 | 5.89 | **7.76** |

*Table 2.4: The change in abundances (central values) from updating the reaction rates. Second column: Reference run, same as last run in table 2.1. Third-eight column: Adding each of the new nuclear rates separately. Ninth column: The effect of including all six updated nuclear rates. All runs were made with the SBBN parameters $\eta_{10} = 6.10$, $N_\nu = 3.046$ and $\tau_n = 880.3$. Note that the reference run in the second column is not the original code, but the one with extended nuclear network from the last column in table 2.1. Thus the value in the second row for each "element box" must not be confused with being the overall change relative to the original code. The overall changes are found in table 2.5.*
** Central abundance value. For $Y_p$ this is relative to the total baryon abundance, while the rest is given relative to the hydrogen abundance.*
*† Change in the abundance relative to the reference run in column two, given in percent.*
*‡ Linearly calculated abundance uncertainty, relative to the central abundance, given in percent.*

| $Y_p$ | $[D/H]_p$ | $[^3He/H]_p$ | $[^7Li/H]_p$ | $[^6Li/H]_p$ | $[^7Be/H]_p$ |
|---|---|---|---|---|---|
| 0.00 | -4.55 | 0.88 | 17.88 | -3.65 | 18.77 |

*Table 2.5: The overall relative changes in the prediction of the primordial abundances for all the updates made to AlterBBN regarding the nuclear network and the reaction rates.*

higher temperatures I follow the suggestion from Serpico et al. 2004 [56] [3] and use the reaction rate from Smith et al. [61].

Finally, I have updated the rates of the $^7Be$ production/destruction reactions $^3He(\alpha,\gamma)^7Be$ [54] (number 27) and $^7Be(n,\alpha)^4He$ [53] (number 19). The authors of both papers have provided best-fit formulas which are used here, and can be found in appendix B. However, the uncertainties for reaction number 19 are evaluated for specific temperatures, restated in table B.1, and extended to a continuous set of temperature ranges in the code. This reaction is not listed in table 2.6, since it is not among the most important reactions for the predictions of the abundances and the uncertainties. However, although it is not important for the predictions of deuterium and helium, it will have a non-trivial effect on the prediction of primordial $^7Li$. The lithium problem can not be explained solely in terms of a "nuclear solution" (see chapter 1.2), but more accurate nuclear reaction rates may shorten the gap between the observed and

[3] This is where the previous rate for the reaction was taken from, also valid only for $T_9 < 1.5$.

the predicted abundance. The $^7Be(n,\alpha)^4He$ reaction is amongst the key sources of $^7Be$ destruction [53], which highly affects the post-BBN $^7Li$ abundance (chapter 1.2). The original *AlterBBN*-adopted rate of this reaction is from Wagoner 1969 [43]. Work done by Hou et al. 2015 [53] suggests that Wagoner overestimates the rate by a factor of ten, and is only to be considered as an upper limit. Experimental results regarding the rate and uncertainty of this reaction are listed in table B.1 in appendix B, together with the best-fit parametric formula used in calculating the reaction rate. As concluded in ref. [53], the new rate is more accurate but worsens the lithium problem by 1.2%.

The effect on the relic abundances from including the new reactions is seen in table 2.4. Be aware that the column marked "Org. rates" is not a run made with the original code, but with the extended nuclear network, seen in the last column in table 2.1. The overall changes in the predictions of the primordial abundances are listed in table 2.5.

### 2.2.5 The Initial Electron-Positron Entropy Density

From equation 2.4 we see that we need to know the entropy density of the $e^{\pm}$-pairs at the starting temperature in order to estimate the initial value of $h_\eta$. In the original code the $e^{\pm}$-pairs are assumed to be highly relativistic at the onset of the calculations, thus the ratio of their entropy density to the photon entropy density is $s_{e^{\pm}}/s_\gamma = 7/4$. For very high starting temperatures this is a very good assumption indeed. However, since it is recommended to start the iterations at around neutrino decoupling (see discussion in section 2.3), a natural starting point is for temperatures in the range $T_{9,i} \sim 20-30$. At 2.0 MeV the entropy ratio is reduced to 6.95/4 [23] since the $e^{\pm}$-pairs have started to become non-relativistic. In the right panel in figure 2.1 the deuterium yield is plotted for different starting temperatures, assuming an instantaneous neutrino decoupling temperature of 2.3 MeV. The blue solid line in the main window is the yield results from using the corrected entropy density, while the results from using the ultra-relativistic assumption is shown as the dashed orange line. The light blue lines on each side of the corrected yields shows the uncertainty in the predictions, while the horizontal band correspond to the observational constraints. There is a $\sim 0.7\%$ increase in the deuterium abundance for $T_{9,i} = 27$, while the difference is slightly larger using lower starting temperatures.

The correction of the initial $e^{\pm}$ entropy density is calculated using the full expressions for their energy density (equation 2.17) and pressure (equation 2.18). These equations need the electron degeneracy parameter $\phi_e$ as input, which again is dependent on $h_\eta$, so we have come to a full circle. However, looking at the left panel in figure 2.1 we see that $\phi_e$ is vanishingly small at the high starting temperatures, and we can safely set this to zero.

## 2.3 Iteration Parameters: General Remarks And Recommended Values

The general consensus is that Big Bang Nucleosynthesis happens between $\sim$ 1 MeV and $\sim$ 70 keV, which are the temperatures of a more or less fully freeze-out of the weak interactions and the end of the deuterium bottleneck respectively. The weak freeze-out is not an abrupt process, and as mentioned in chapter 1.1.6, the freeze-out process starts already at temperatures $\sim 2-3$ MeV. Enqvist et al. [62] recommend using $T_{\nu d} = 2.3$ MeV for the decoupling temperature when assuming instantaneous neutrino decoupling. Starting the iteration at the time of neutrino decoupling simplifies some of the physics implemented in the program, so I have decided to use $T_{9,i} = 27$ as the initial temperature for the calculations in this project. In chapter 3 we will discuss the results of Nollett & Steigman [48] [25] in the light of the implementation of light WIMPs in *AlterBBN*, and their calculations are based on an instantaneous neutrino decoupling temperature of $T_{\nu d} = 2.0$ MeV. Although the effect is very small, we see in the right panel of figure 2.1 that the resulting deuterium abundance is somewhat sensitive to the starting temperature. For unknown reasons the uncertainty seems to fluctuate a bit for differing initial temperatures,

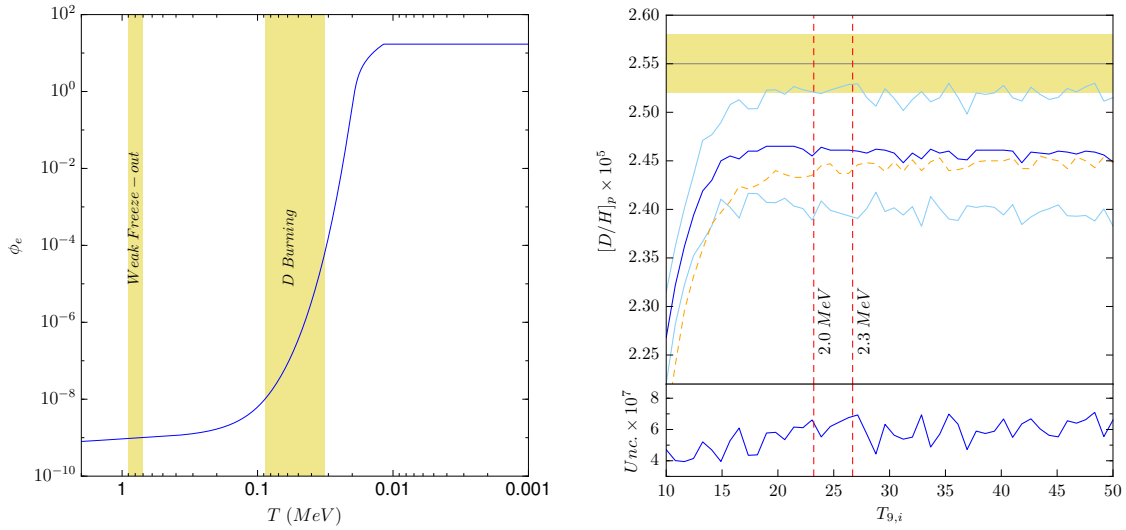


*Figure 2.1: Left panel: The electron degeneracy parameter $\phi_e = m_e/T_9$ plotted against the temperature, with the colored vertical bands corresponding to the times of weak n/p freeze-out and deuterium burning (effective BBN) respectively. Right panel: The deuterium yield, plotted for different initial temperatures, assuming instantaneous neutrino decoupling at $T_{\nu d} = 27$ (∼2.3 MeV) and SBBN. The blue solid line in the upper window is the yield from using the corrected $e^{\pm}$ entropy density, while the dashed orange line is for the assumption of highly relativistic $e^{\pm}$-pairs. The lighter blue lines show the uncertainty in the predictions, which is also plotted in the bottom window. The horizontal band is the observed constraint on the primordial deuterium abundance.*

tending towards lower uncertainties for lower starting temperatures. This is shown in the bottom window in the right panel of the figure. At around 15 MeV the electrons and positrons start annihilating, and one should avoid starting any later than this, as it would underestimate the expansion rate.

There are good reasons not to start the integration process even earlier, aside from the obvious fact that the computational time goes down, and that not much of importance happens when all the BBN-relevant particles are still in thermodynamic equilibrium. Starting at e.g. $T_{9,i} \sim 100$ the muons may still be semi-relativistic ($m_\mu = 105.7$ MeV) and not fully annihilated. This introduces extra relativistic degrees of freedom and a potential error when employing entropy conservation in finding the initial value of $h_\eta$ (equation 2.4). At the time of weak freeze-out, the mouns have become fully non-relativistic, and we don't have to take them into account. In the scenario of including light WIMPs it is necessary to deal explicitly with neutrino decoupling, and it is therefore convenient to start the iterations right after neutrino decoupling. Also in the standard scenario it is a useful assumption, since it simplifies the set of equations governing the iteration. Knowing this is crucial in the case where the user would want to start the iterations at a higher temperature. Not only is $\eta$ found by conservation of entropy at the time of neutrino decoupling, but the expression for the neutrino energy density is based on the assumption that $T_\nu \propto a^{-1}$, which is strictly true only after the neutrinos have decoupled. In the case of a neutrino coupled WIMP, however, it was necessary to promote $T_\nu$ to a dynamic variable, similar to $T_9$, since the annihilation of the WIMP will heat the neutrinos relative to the photons. The necessary changes in this case are discussed in chapter 3.

The initial temperature may be changed by the user through the *.ini* input-file, but I have found no reason to include this option for the final temperature. I have set this to $T_{9,f} = 0.01$, which corresponds to ∼ 1 keV. By this time the BBN has ended in earnest, and the light element abundances have frozen out (except from the decay of $^3H$ and $^7Be$ into $^3He$ and $^7Li$ respectively).

In the main function *nucl* a set of iteration parameters that controls the adaptive step-size for the Runge-Kutta driver are defined. Each time-step is determined by the requirement that the abundances and temperature do not change too much, and the controlling parameters are

- CY - the maximum change in the abundances, $(dY/dt)_{max}$;
- CT - the maximum change in the temperature, $(dT/dt)_{max}$;
- DT0 - initial time-step;
- NITMAX - maximum number of recorded iterations;
- INC - maximum number of increments before recording.

It is important to have a set of parameters which ensures that the iteration process runs all the way from the initial to the final temperature, otherwise the iteration may stop before the BBN has ended. As a default, the original program uses the values $CY = 0.1$, $CT = 0.01$, $DT0 = 10^{-4}$, $NITMAX = 1000$ and $INC = 50$ for the calculation of the abundances. However, for the uncertainty estimation the default values are $CY = 0.5$, $CT = 0.1$, $DT0 = 10^{-2}$, and $NITMAX = 10$, keeping INC unaltered. If the uncertainties computed in the default scenario do not satisfy some specified conditions, the function *nucl_failsafe* "kicks" in. This function is a copy of the function *nucl*, except that the iteration parameters are adjusted to the values they have for the abundance calculation. In my view, the conditions for activating *nucl_failsafe* is too conservative if one is interested in getting a good estimate of the uncertainties. Comparing runs where the default iteration parameters are used, with runs where the uncertainties are analyzed with the same time-steps as for the abundance calculation, the resulting uncertainties may differ by several percent. For this reason, when the uncertainties are of interest, I will use the same set of iteration parameters for both the abundance and uncertainty calculation. This way, we ensure that they are analyzed at the same points. When only the abundances are of interest, the default values may just as well be used to shorten the computation time.

## 2.4 Discussion

With the updates and changes of *AlterBBN* there have been a significant decrease in the predicted deuterium abundance. In the original code this was estimated to $[D/H]_p = 2.573 \pm 0.036 \cdot 10^{-5}$ assuming SBBN, while the updated *AlterBBN* have seen this drop by $\sim 4.5\%$ to $2.456 \pm 0.057 \cdot 10^{-5}$, still just within the suggested observational constraint of $2.55 \pm 0.03 \cdot 10^{-5}$. We also note that the lithium problem is worsened, with a major increase in both the relic $^7Li$ and $^7Be$ yields. The $^4He$ abundance was not affected at all, still being $Y_p = 0.2472 \pm 0.0001$, which is within the suggested observational constraint of $0.2449 \pm 0.004$. Except for $^4He$ and $^6Li$ there have been an overall increase in the uncertainties, with the uncertainty in the deuterium prediction now being 2.3%, mainly arriving from the extended nuclear network and the rates for the reactions $D(p,\gamma)^3He$, $D(D,n)^3He$ and $D(D,p)^3H$ from Coc et al. [55]. It is evident that accurate nuclear rates are essential for predicting the light element abundances, as we have seen significant impacts on the predictions and the uncertainties only by updating six of the reaction rates.

Since the initial value of several of the parameters needed in the iteration relies on entropy conversion at the time of neutrino decoupling, it is recommended to start the iterations here. In relaxing the assumption of ultra-relativistic $e^{\pm}$-pairs at the corresponding temperatures, we found an increase by $\sim 0.7\%$ in the resulting deuterium yield, with a minor dependence on the initial temperature.